

Article

A Novel Wind Turbine Concept Based on an Electromagnetic Coupler and the Study of Its Fault Ride-through Capability

Rui You ¹, Braulio Barahona ², Jianyun Chai ^{1,*} and Nicolaos A. Cutululis ²

¹ State Key Laboratory of Control and Simulation of Power System and Generation Equipments, Department of Electrical Engineering, Tsinghua University, Beijing 100084, China; E-Mail: you-r10@mails.tsinghua.edu.cn

² Department of Wind Energy, Technical University of Denmark, Risø Campus, Frederiksborgvej 399, Roskilde 4000, Denmark; E-Mails: brauliobarahona@gmail.com (B.B.); niac@dtu.dk (N.A.C.)

* Author to whom correspondence should be addressed; E-Mail: chaijy@mail.tsinghua.edu.cn; Tel.: +86-10-6277-5559; Fax: +86-10-6278-2296.

Received: 13 August 2013; in revised form: 11 October 2013 / Accepted: 13 November 2013 / Published: 22 November 2013

Abstract: This paper presents a novel type of variable speed wind turbine with a new drive train different from the variable speed wind turbine commonly used nowadays. In this concept, a synchronous generator is directly coupled with the grid, therefore, the wind turbine transient overload capability and grid voltage support capability can be significantly improved. An electromagnetic coupling speed regulating device (EMCD) is used to connect the gearbox high speed shaft and synchronous generator rotor shaft, transmitting torque to the synchronous generator, while decoupling the gearbox side and the synchronous generator, so the synchronous generator torque oscillations during a grid fault are not transmitted to the gearbox. The EMCD is composed of an electromagnetic coupler and a one quadrant operation converter with reduced capability and low cost. A control strategy for the new wind turbine is proposed and a 2 MW wind turbine model is built to study the wind turbine fault ride-through capability. An integrated simulation environment based on the aeroelastic code HAWC2 and software Matlab/Simulink is used to study its fault ride-through capability and the impact on the structural loads during grid three phase and two phase short circuit faults.

Keywords: variable speed wind turbine; electromagnetic coupler; synchronous generator; voltage support capability; HAWC2; structural loads

1. Introduction

Wind energy has great potential of development and utilization for its pollution-free and renewable characteristics. Wind turbine technology has undergone tremendous development in recent years. The earliest wind turbine design is the constant-speed constant-frequency (CSCF) wind turbine. The squirrel cage induction generator is used for grid connection. Though it has the benefits of a simple structure and high robustness, the almost constant rotor speed regardless of the wind speed results in the low power coefficient and high mechanical stress. Furthermore, capacitors must be added to compensate the reactive power absorbed by the induction generator and improve the grid power factor. Nowadays, the mainstream wind turbine concept is the variable-speed constant-frequency (VSCF), in which the rotor speed can change according to different wind speeds, therefore, a maximal wind power capture can be achieved. This can also result in smoother output power [1,2].

The most common VSCF wind turbines nowadays are Type 3 and Type 4 wind turbines [3]. The stator is directly connected to the grid and only slip power goes through the converter for the doubly fed induction generator (DFIG) in Type 3 wind turbine. This allows for rating the converter to a fraction of the rated power [4], but the necessary gearbox results in the high cost and the need for regular maintenance. In Type 4 wind turbine, all the synchronous generator output power is delivered through a converter, therefore, though a gearbox is not necessary, the full scale converter increases the cost significantly with the increased wind turbine power ratings [5–7].

With the rapid increase of the wind power levels in the power system, requirements of wind turbine fault ride-through (FRT) capability have been introduced in different countries [8]. The voltage profile requirements are given specifying the depth of the voltage drop and the clearance time as well. The fault duration varies from 100 ms to 625 ms, whereas the voltage drop down level varies from 25% to even 0% of the nominal value. Moreover, 100% reactive current injection is required in some countries like Germany for better grid voltage recovery.

Compared with the synchronous generators widely used in conventional power plants, the two most common types of VSCF wind turbines have weaker transient overload capability, FRT performances and grid voltage support capability [9–12]. In this paper, a variable speed wind turbine based on electromagnetic coupler (WT-EMC), with a new drive train, is proposed. A synchronous generator is directly coupled with the grid, so the compatibility between this wind turbine and the power system can be effectively improved.

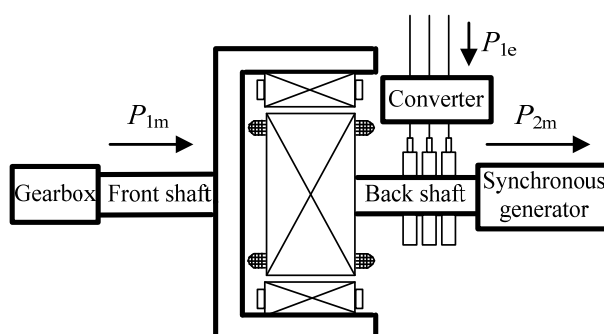
The paper is organized as follows: Section 2 introduces the WT-EMC concept, particularly the structure of the key device, the electromagnetic coupling speed regulating device (EMCD); Section 3 presents the control strategy of WT-EMC; Section 4 proposes a model of WT-EMC and the electromagnetic coupler model is detailed; a case study of the influence on electrical performance and wind turbine structural loads during grid three phase and two phase faults is presented using Matlab/Simulink and HAWC2 software tools; and Section 5 concludes the analysis.

2. Concept of WT-EMC

In this wind turbine concept, a synchronous generator is directly coupled with the grid, therefore, its speed is almost constant once it is connected to grid. However, the wind turbine main shaft speed

changes according to the different wind speeds, so a device is necessary to connect the two shafts rotating with different speeds—the main shaft and the synchronous generator rotor shaft—and transmit the torque from the main shaft side to the synchronous generator side. For example, in [13], a hydro-dynamically controlled gearbox is described as such a device. In this paper, the EMCD is proposed. Because of the large speed difference between the main shaft and the synchronous generator rotor shaft, a gearbox is necessary in the drive train. The typical structure of an EMCD is shown in Figure 1. It is composed of an electromagnetic coupler and a converter. The electromagnetic coupler is essentially a squirrel induction motor with two revolving shafts connected with the gearbox and synchronous generator. The converter controls the electromagnetic coupler speed and electromagnetic torque. During wind turbine operation, the front shaft speed is always lower than the back shaft speed and the power through the converter is only a small fraction of the wind turbine rated power—1/6 of the wind turbine rated power in this paper [14]. In this way, only a one quadrant operation converter and a gearbox with lower gear ratio compared with Type 3 wind turbine are needed, resulting in a lower cost. The converter characteristics above and the squirrel induction motor characteristic robustness make the EMCD highly reliable.

Figure 1. Schematic diagram of the electromagnetic coupling speed regulating device's (EMCD) typical structure.



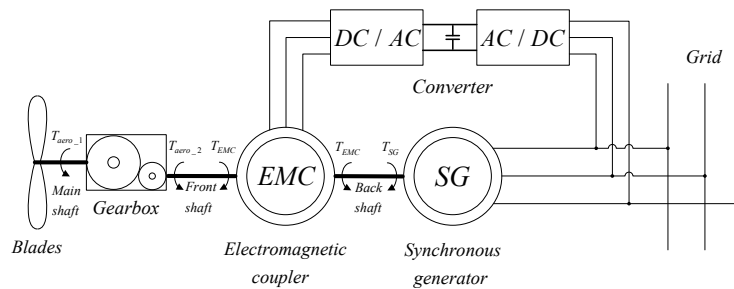
Since it acts as the medium drive stage, the EMCD power transmission relationship is very different from that of a normal induction motor. The input power is from the mechanical power P_{1m} of the front shaft and the electrical power P_{1e} of the converter. Both mechanical and electrical losses are included. The mechanical loss includes the frictional losses both in the front and back shafts, while the electrical loss is the sum of the electromagnetic coupler and converter losses. The output power P_{2m} is the synchronous generator input mechanical power. The ratio between the output power and input power is the EMCD transmission efficiency η_{EMCD} shown in Equation (1):

$$\eta_{EMCD} = P_{2m}/(P_{1m} + P_{1e}) \quad (1)$$

The transmission efficiency was calculated on a 30 kW experimental platform, where it was found to reach up to 95% around the rated condition [15]. A scaled up electromagnetic coupler that can be used in a 1.5 MW WT-EMC has been built and incorporated in an experimental platform which is similar to the one described in [15]. The experiments are ongoing, so final results are not yet available, but the preliminary results indicate that the electromagnetic coupler transmission efficiency can reach 98%. Furthermore, the length is 2.5 m and weight is 6.5 ton for the built electromagnetic coupler used in 1.5 MW WT-EMC. Based on those metrics, preliminary calculations indicate that a 1.5 MW wind

turbine with the proposed drive train should have a cost comparable to the Type 3 wind turbine with same power rating. The WT-EMC structure is shown in Figure 2. The blades capture the wind power and apply the aerodynamic torque T_{aero_1} on the low speed shaft of gearbox. If the gearbox is treated ideal and its speed ratio is set to n , the torque applied on the front shaft is $T_{aero_2} = T_{aero_1} / n$.

Figure 2. Schematic diagram of the wind turbine based on electromagnetic coupler's (WT-EMC) structure.



The front shaft speed ω_f and back shaft speed ω_b are calculated below:

$$\begin{aligned} T_{aero_2} - T_{EMC} - B_f \omega_f &= J_f \frac{d\omega_f}{dt} \\ T_{EMC} - T_{SG} - B_b \omega_b &= J_b \frac{d\omega_b}{dt} \end{aligned} \quad (2)$$

where T_{EMC} is the electromagnetic torque of the electromagnetic coupler applied by the converter; T_{SG} is the synchronous generator electromagnetic torque; J_f and J_b are the front shaft moment of inertia and back shaft moment of inertia, respectively; B_f and B_b are the front shaft friction factor and back shaft friction factor, respectively. The aeroelastic wind turbine model and electromagnetic coupler dynamic model will be detailed in Section 4.

Because only the back shaft contributes to the inertia, the synchronous generator used in this wind turbine has less inertia compared with the synchronous generators used in conventional power plants. However, the synchronous generator inherent inertial response capability contributes to the frequency stabilization, *i.e.*, when the frequency drops due to some sudden change of generation and load, the synchronous generator rotor speed decreases and the kinetic energy of back shaft is delivered to grid. Therefore, the frequency regulation performance for this wind turbine is better than Type 3 and Type 4 wind turbines which do not have a natural inertial response to changes of the grid frequency, but it has to be emulated. T_{EMC} is applied by the converter, so the quick change of the torque applied on the synchronous generator rotor can be achieved. Because the converter is supplied from the grid, when the grid voltage is too low the torque T_{EMC} that the converter can apply is limited. These are the main differences between the synchronous generator used in this wind turbine and synchronous generators used in conventional power plants.

3. Operation Modes and Control Strategies of WT-EMC

This section describes control strategies of WT-EMC during essential normal operation modes such as start and synchronization, operation after grid connection, grid disconnection and stop and FRT and synchronous condenser modes.

3.1. Normal Operation Modes

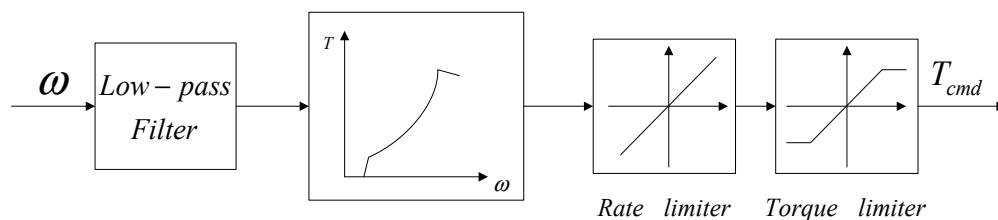
3.1.1. Start and Synchronization

Due to the two separate shafts—the front shaft and the back shaft shown in Figures 1 and 2—the wind turbine start process is different from that of normal wind turbines. The start process can be divided into two steps: synchronous start and asynchronous start. At first the pitch angle β decreases to increase aerodynamic torque and the main shaft accelerates gradually. At the same time the converter operates in speed control mode to control the back shaft speed such that it rotates synchronously to the front shaft until its speed reaches a certain value below the synchronous speed (80% of the synchronous speed in this paper). This is the synchronous start process. Then the asynchronous start process starts. The front shaft speed is kept quasi-constant by pitching the blades, while the back shaft is gradually accelerated to a speed slightly higher than the synchronous speed (100.2% of the synchronous speed in this paper) using the converter. Once this is accomplished, the excitation voltage is applied for the synchronization. A grid connection device dynamically adjusts the excitation voltage and the converter output frequency according to the measured voltage and phase differences between the synchronous generator and grid. When the measured voltage and phase differences are within the synchronization range, the grid connection switch is closed automatically and the control mode of converter is switched from the speed control mode to the torque control mode immediately to maximize the wind power captured by regulating the converter torque command explained below.

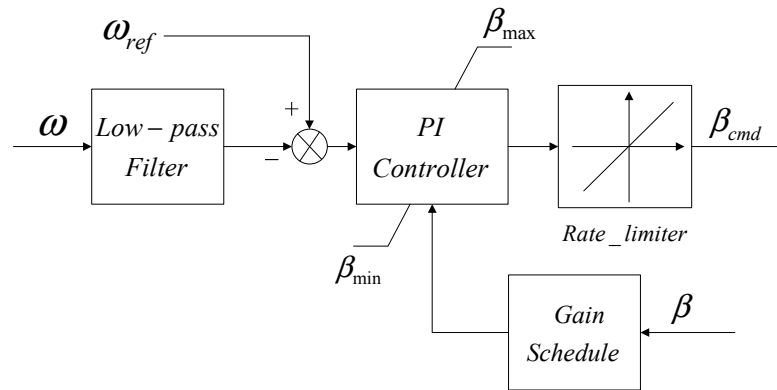
3.1.2. Operation after Grid Connection

The converter torque command T_{cmd} and the pitch angle command β_{cmd} are calculated in a manner similar to Type 3 and Type 4 wind turbine, as shown in Figures 3 and 4, respectively. However, in the grid connection operation, the converter torque command should increase gradually from almost zero to the value T_{cmd} calculated according to the current wind speed conditions, as described in Figure 3. The torque reference is calculated from the torque-speed characteristic, using as input the filtered main shaft speed. Then the torque command T_{cmd} is calculated, taking into account rate and torque limits [4].

Figure 3. Schematic diagram of converter torque command calculation.



The pitch angle controller, shown in Figure 4, uses a speed signal as the input signal to a proportional-integral (PI) controller. Finally, a gain-scheduling block will adapt the gain according to the current pitch angle β to compensate for the existing non-linear aerodynamic characteristics [16].

Figure 4. Schematic diagram of pitch angle controller.

3.1.3. Grid Disconnection and Stop

To stop the wind turbine, the converter gradually decreases the torque to zero, when the grid connection switch is opened. At this moment, the converter is switched to the speed control mode.

Like the start process, there are also two steps in the stop process: asynchronous stop and synchronous stop. With the change of the pitch angle, the front shaft speed is kept at quasi-constant speed, equal to the value when the grid connection switch was opened. The back shaft gradually decelerates to the same speed as the front shaft with the change of the converter speed command. This is the asynchronous stop process. When the two shafts rotate at the same speed, they gradually decelerate to zero with the increase of pitch angle and the synchronous stop process finishes.

3.2. FRT and Synchronous Condenser Modes

In case of severe grid fault operation conditions, the converter torque command T_{cmd} is changed to zero suddenly and the converter is controlled to block the pulse width modulation (PWM) output to decouple the synchronous generator and the gearbox side drive train. In order to prevent the wind turbine from going into overspeed, pitching in advance may be needed. After the grid fault, the converter is restarted and its torque command should gradually increase to the value T_{cmd} calculated in Figure 3. If the grid fault is not severe and the converter input voltage is within its allowable voltage range, the converter operates normally but the torque command should be adjusted according to the synchronous generator terminal voltage. If the synchronous generator terminal voltage is k per unit (pu) which is less than one and the torque command calculated in Figure 3 is T_{cmd} , the torque command during the grid fault should be kT_{cmd} in order to keep the synchronous generator output active current almost constant. The synchronous generator excitation voltage is regulated to change the reactive power generated for grid voltage support.

WT-EMC can also be used to regulate its output reactive power even at zero active power. That means that when the wind speed is very low, the pitch angle can be kept around 90 degrees and the wind turbine rotor does not rotate. With the change of the converter speed command from 0% to 100.2% of the synchronous speed, the speed preparation for the grid connection will be ready. After the other grid connection requirements are fulfilled, the grid connection can be finished. Then the converter control mode is switched immediately from speed to torque mode. The torque command is kept around zero and the synchronous generator is used as a synchronous condenser. By changing the synchronous

generator excitation voltage the wind turbine reactive power generated can be regulated according to the grid command or the synchronous generator terminal voltage. Compared with common wind farms, the reactive power compensation devices can be saved, so the related wind farm costs are reduced, while wind farm capability to support power system is improved.

4. Simulation of WT-EMC FRT Capability

This section first describes the electromagnetic coupler and synchronous generator models. Then the WT-EMC model built in an aeroelastic code and Matlab/Simulink is presented. A case to study the FRT capability is proposed and finally the simulation results are analyzed.

4.1. Electromagnetic Coupler and Synchronous Generator Dynamic Models

The two shafts both rotate for the electromagnetic coupler. In spite of this, the shaft connected with synchronous generator is called stator and the shaft connected with gearbox is called rotor in the model below for a better comparison with normal squirrel induction motor. Represented in the dq coordinates, the electromagnetic coupler fluxes equations are [17]:

$$\begin{aligned}\psi_{sd} &= L_s i_{sd} + L_m i_{rd} \\ \psi_{sq} &= L_s i_{sq} + L_m i_{rq} \\ \psi_{rd} &= L_m i_{sd} + L_r i_{rd} \\ \psi_{rq} &= L_m i_{sq} + L_r i_{rq}\end{aligned}\quad (3)$$

where ψ_{sd} and ψ_{rd} are the d -axis stator flux and rotor flux, respectively; ψ_{sq} and ψ_{rq} are the q -axis stator flux and rotor flux, respectively; L_m , L_s and L_r are the mutual inductance between the stator and rotor, the self inductance of stator and the self inductance of rotor, respectively; i_{sd} and i_{rd} are the d -axis stator current and rotor current, respectively; and i_{sq} and i_{rq} are the q -axis stator current and rotor current, respectively. The electromagnetic coupler voltages equations are:

$$\begin{aligned}u_{sd} &= R_s i_{sd} + p\psi_{sd} - \omega_1 \psi_{sq} \\ u_{sq} &= R_s i_{sq} + p\psi_{sq} + \omega_1 \psi_{sd} \\ 0 &= R_r i_{rd} + p\psi_{rd} - (\omega_1 - \Delta\omega)\psi_{rq} \\ 0 &= R_r i_{rq} + p\psi_{rq} + (\omega_1 - \Delta\omega)\psi_{rd}\end{aligned}\quad (4)$$

where u_{sd} and u_{sq} are the d -axis stator voltage and q -axis stator voltage, respectively; p is the differential operator; R_s and R_r are the stator resistance and rotor resistance, respectively; ω_1 is the synchronous electric angular velocity; and $\Delta\omega$ is the electric angular velocity difference between the back shaft and front shaft. The electromagnetic torque T_{EMC} is:

$$T_{EMC} = \frac{n_p L_m}{L_r} (i_{sq} \psi_{rd} - i_{sd} \psi_{rq}) \quad (5)$$

where n_p is the number of pole pairs.

The electromagnetic coupler model is almost the same as the normal squirrel induction motor. The only difference is that $\Delta\omega$ is used to replace the rotor electric angular velocity in the normal

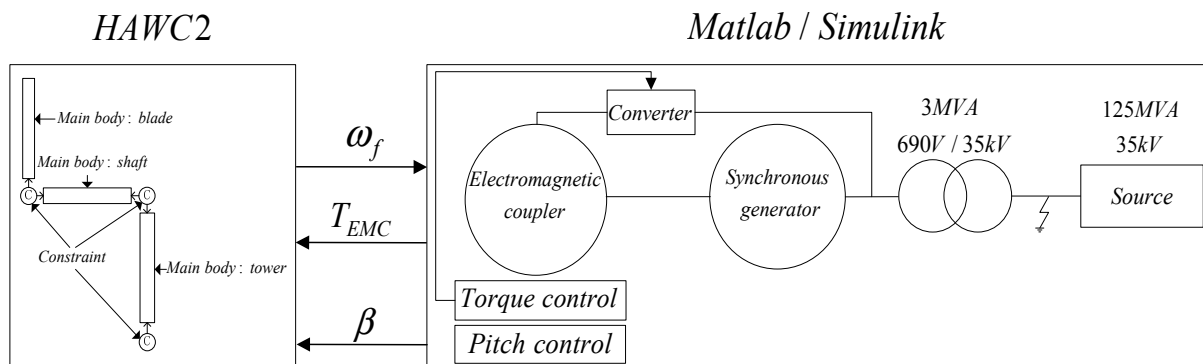
squirrel induction motor model. This is because there are two rotation shafts in the electromagnetic coupler and the angular velocity difference between them amounts to the normal squirrel induction motor angular velocity.

The synchronous generator model is a classical sixth-order state-space model [18]. The model takes into account the dynamics of the stator, field, and damper windings. The magnetic saturation is ignored, so the relationship between field current and terminal voltage is linear. The excitation system is modeled as a direct current (DC) exciter, described in [19].

4.2. Wind Turbine Model for Numerical Simulations

The proposed model of WT-EMC is shown in Figure 5. The aeroelastic, structural and mechanical aspects are simulated in the state-of-art HAWC2 software developed at Technical University of Denmark (DTU) Wind Energy [20,21]. HAWC2 is an aeroelastic simulation code, which provides an advanced model for the flexible structure of wind turbines based on a multibody formulation. The mechanical components (*i.e.*, blades, shafts, tower) are each composed of many Timoshenko beam elements. The aeroelastic model corresponds to a 2 MW wind turbine with rotor diameter of 80 m and tower height of 80 m.

Figure 5. Schematic diagram of simulation model.

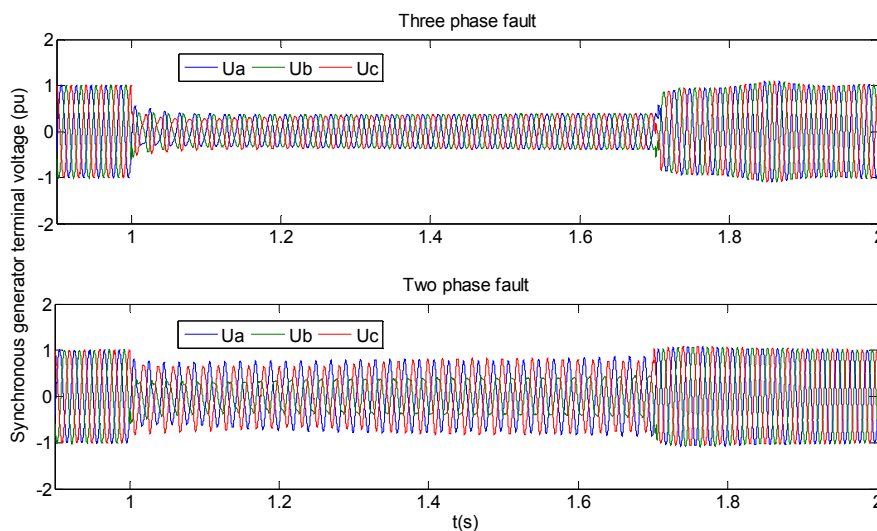


The electrical components are simulated in Matlab/Simulink. The synchronous generator rated at 2.5 MVA, 690 V, 1500 rpm is connected to a 35 kV, 125 MVA network through a 3 MVA transformer. The rated speed of the electromagnetic coupler shaft connected to gearbox is 1350 rpm. The synchronous generator excitation system regulates the excitation voltage to keep the terminal voltage around the rated voltage. The converter is supplied from the synchronous generator terminal 690 V bus and applies the electromagnetic torque T_{EMC} , which is the synchronous generator input mechanical torque.

4.3. Simulation Results

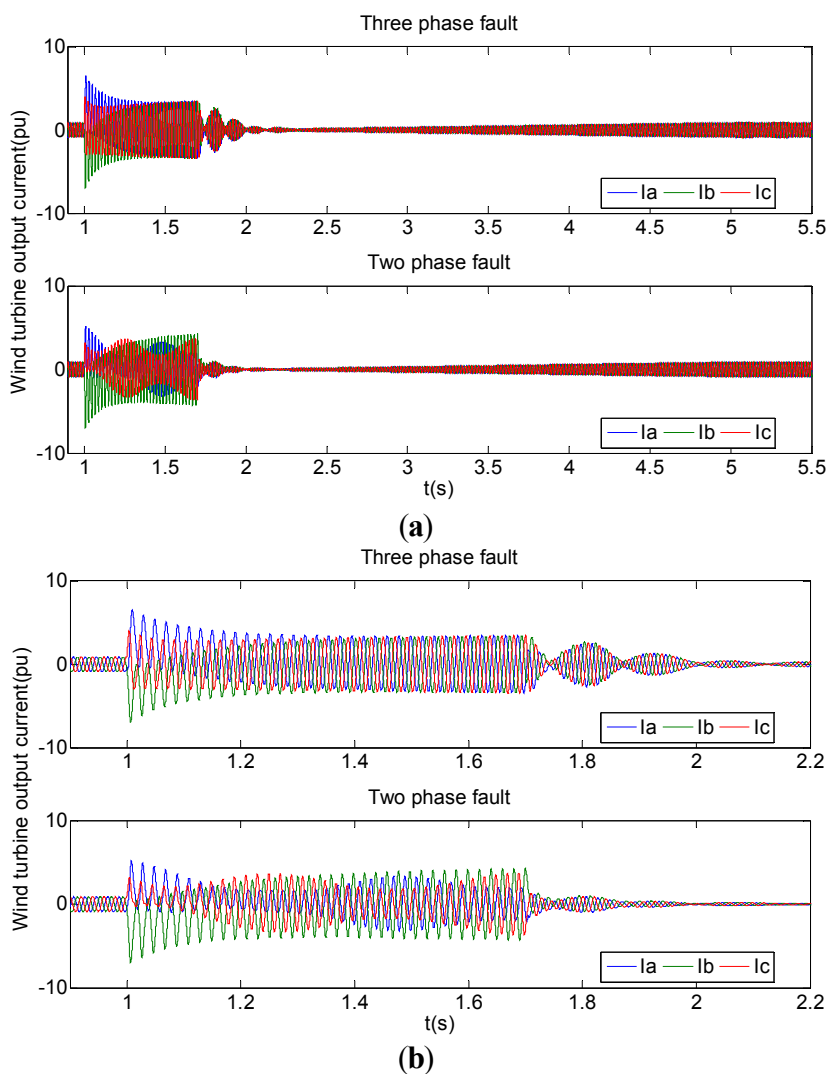
In order to study the FRT capability of WT-EMC, three phase and two phase short circuit faults are simulated to occur on the 35 kV bus at 1 s, and the faults are cleared after 0.7 s. Compared with the requirements in [8], the faults simulated in this paper are more severe than any of them in terms of voltage dip and fault duration. The wind speed is set constant, above rated, at 15 m/s. In order to show the whole dynamic change process of the simulated signals, different time frames are used in the figures below. The synchronous generator terminal voltages are shown in Figure 6.

Figure 6. Synchronous generator terminal voltage.



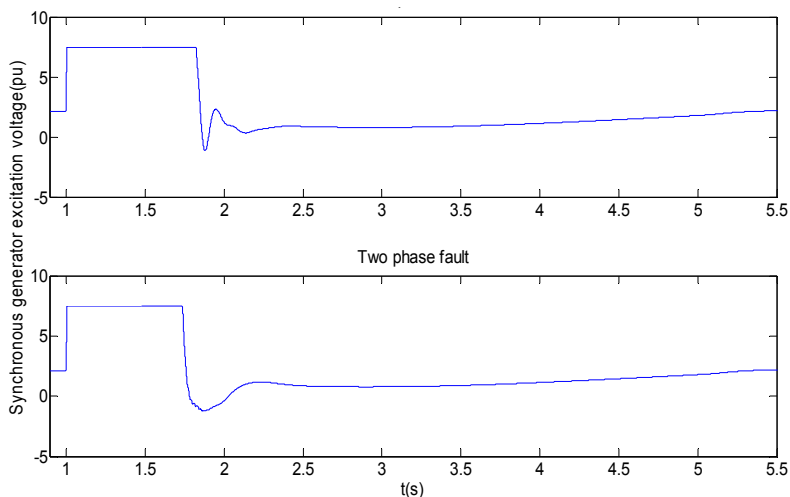
The wind turbine total output three phase currents are shown in Figure 7. Figure 7b is a zoom of Figure 7a during 0.9 s and 2.2 s.

Figure 7. Wind turbine output current (a) 0.9–5.5 s; and (b) 0.9–2.2 s.



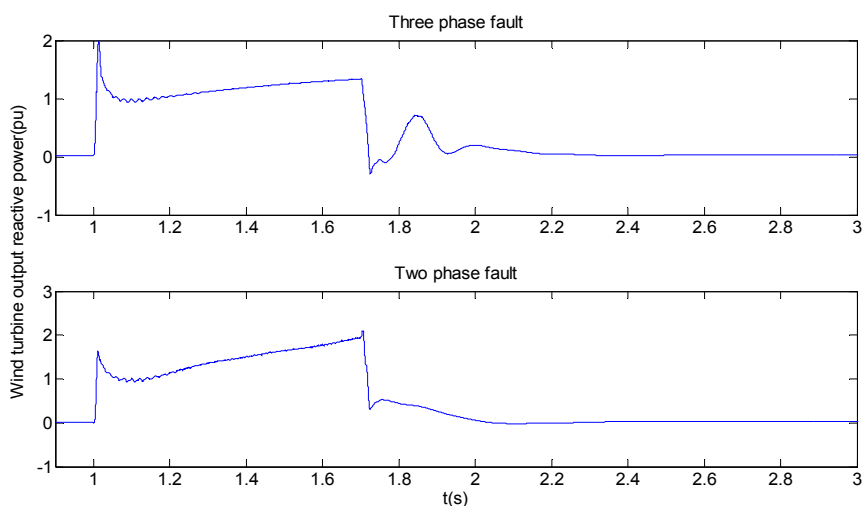
During the fault the excitation system increases excitation voltage to support the synchronous generator terminal voltage. The maximal excitation voltage is set at 7.5 pu and the synchronous generator excitation voltage is shown in Figure 8.

Figure 8. Synchronous generator excitation voltage.



The wind turbine output reactive power is shown in Figure 9. During the fault, the synchronous generator generates only reactive power. The current shown in Figure 7 during the grid fault is only the reactive current which can reach values of up to three times the rated, in order to support the synchronous generator terminal voltage. After the fault is cleared, the reactive power generated decreases to the original value zero to keep the wind turbine power factor at one.

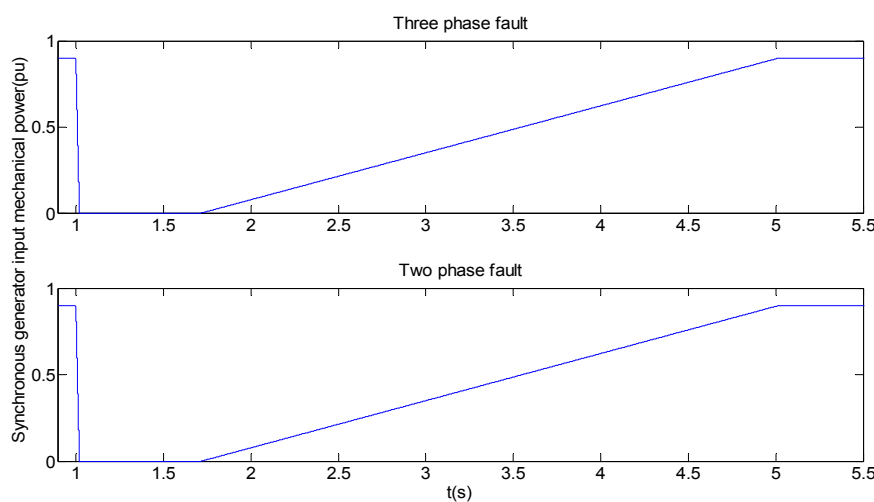
Figure 9. Wind turbine output reactive power.



The wind speed is above the rated speed, therefore, the front shaft speed is at its rated value, 1350 rpm. Because of the synchronous generator capability and the wind turbine power flow relationship, the synchronous generator input mechanical power is 0.89 pu before the grid fault. When the fault occurs, because of the low synchronous generator terminal voltage, the converter is controlled to block its PWM output during the fault. After the recovery of the grid voltage the converter can apply the torque of electromagnetic coupler T_{EMC} and it recovers gradually to the original value. The synchronous generator

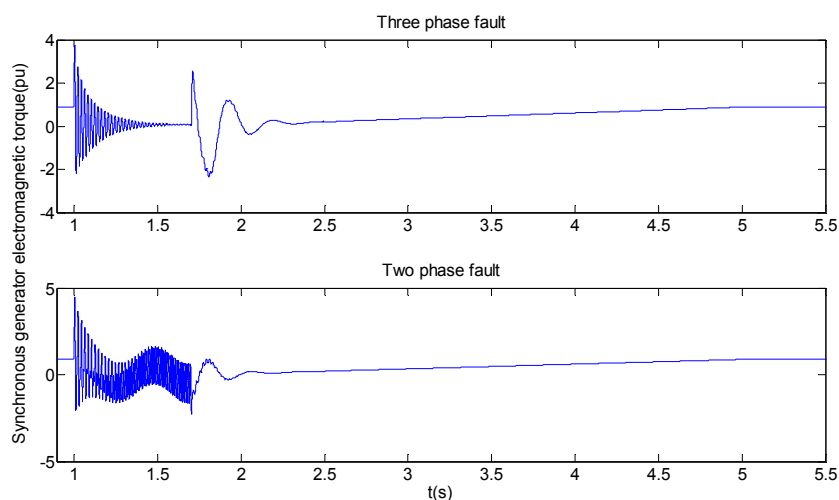
input mechanical power is shown in Figure 10. The increase of the synchronous generator input mechanical power after the grid fault is within 3.3 s—from about 1.7 s to 5 s. This recovery time meets the active power recovery requirement in Germany [22], in which it is stated that “the active power infeed must be increased to the original value with a gradient of at least 10% of the rated generator power per second”. The recovery of the synchronous generator input mechanical power results in the active current gradual increase from 0 to the original value after the grid fault shown in Figure 7. After around 5 s, the wind turbine output current recovers to the steady state value before the grid fault.

Figure 10. Synchronous generator input mechanical power.



The synchronous generator electromagnetic torque is shown in Figure 11. As expected, during the fault, torque oscillations can be seen. Nevertheless, those oscillations are not transmitted further down the drive train, since the electromagnetic coupler can fully decouple the synchronous generator from the gearbox side drive train.

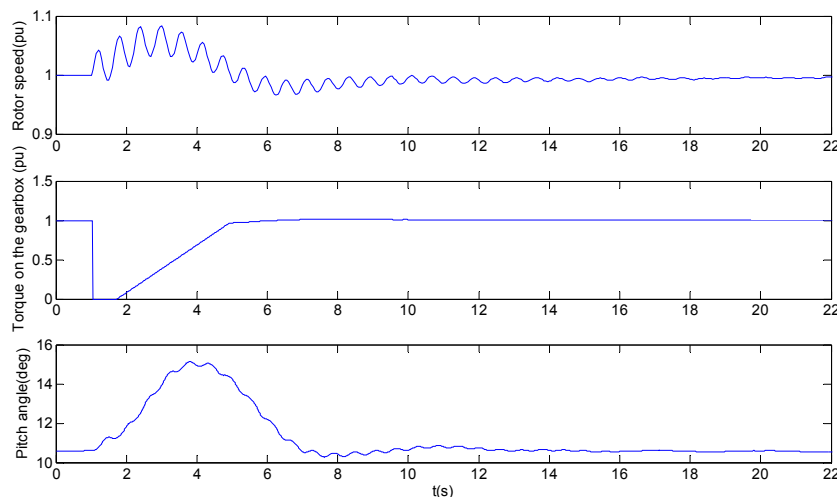
Figure 11. Synchronous generator electromagnetic torque.



The wind turbine rotor speed, torque on the gearbox high speed shaft T_{EMC} and pitch angle are shown below. Because for both three phase and two phase grid faults the torque T_{EMC} signals are the same, as shown in the middle of Figure 12, only one curve is plotted for both faults in all figures below.

Due to the sudden decrease of T_{EMC} , the rotor will start accelerating, at a slower pace, due to the wind turbine inertia. The rotor acceleration is counteracted by the pitch control, avoiding the wind turbine overspeeding, which can cause high inertial loads on the blades.

Figure 12. Rotor speed, torque on the gearbox high speed shaft and pitch angle.



The shaft bending moments, tower bottom bending moments, tower top bending moments and one of the three blades root bending moments (M_x , M_y and M_z) are shown in Figures 13–16. In order to qualitatively assess the impact of the fault on the wind turbine structural loads, these plots include simulation of normal operation (blue) and simulation during the grid fault (red). Compared with the normal operation, the structural loads which are influenced most are shaft torsion moment M_z (bottom plot in Figure 13); tower bottom tilt moment M_x and side-to-side moment M_y (top and middle plot in Figure 14); and tower top tilt moment M_x and side-to-side moment M_y (top and middle plot in Figure 15). Shaft torsion and tower side-to-side moments are directly influenced by the changes of torque on the gearbox high speed shaft, whereas tilt moments are mainly influenced by the actions of the pitch control. Similarly, the different blade root bending moments compared to normal operation result partly from the changes of the torque applied on the gearbox high speed shaft, but mainly from the pitch angle changes applied by the control to maintain the main shaft speed to the rated value.

Figure 13. Shaft bending moments.

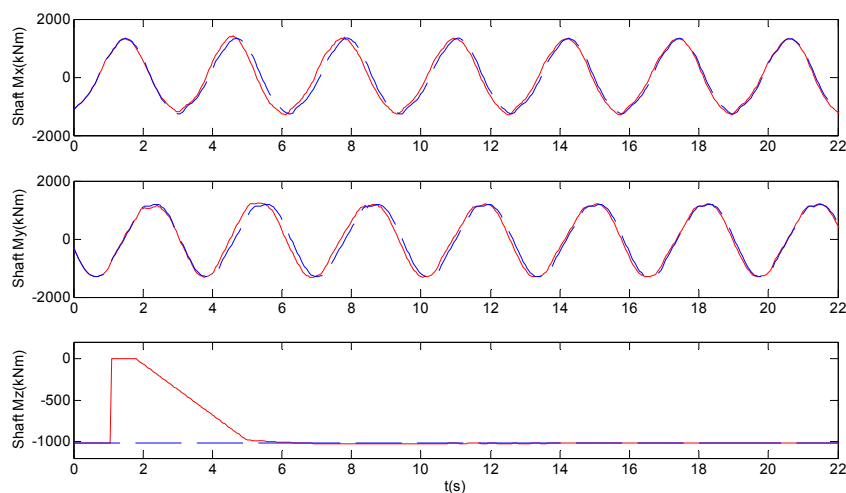


Figure 14. Tower bottom bending moments.

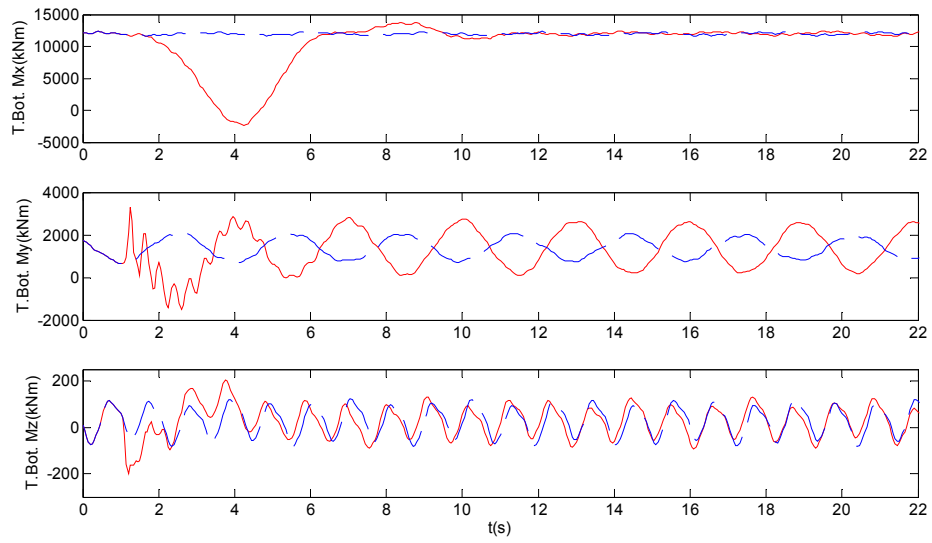


Figure 15. Tower top bending moments.

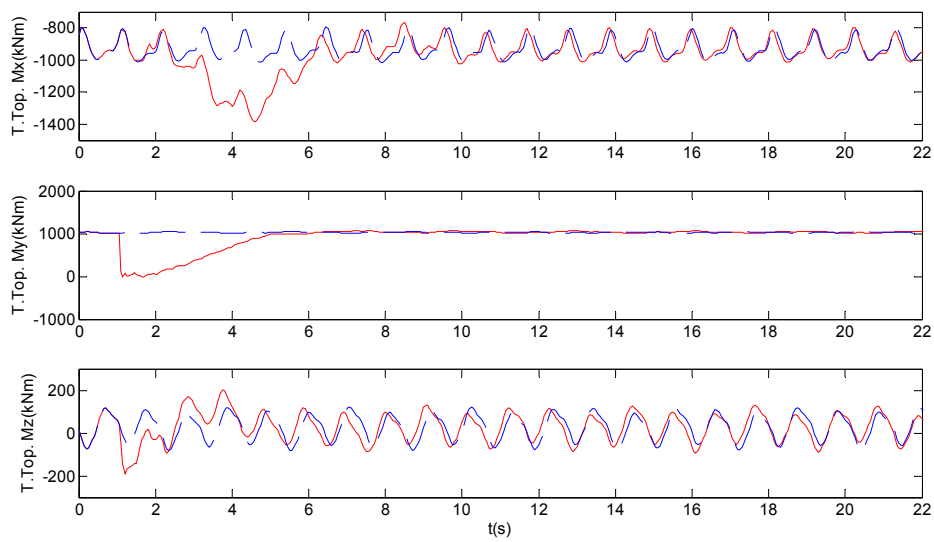
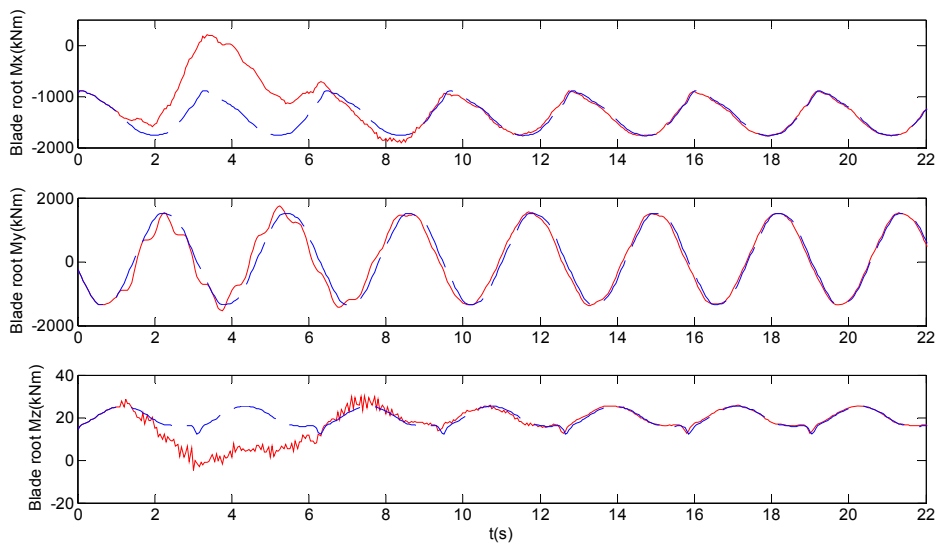


Figure 16. Blade root bending moments.



Furthermore, in comparison with a Type 3 wind turbine, the impact on the drive train during unbalanced grid faults is much less. Because the torque oscillations induced through the fluxes of the DFIG stator in cases of unbalanced faults [23], are not there in the proposed WT-EMC. This contributes to the improvement of the shaft torsion moment and side-to-side moments of tower bottom and tower top, therefore, the drive train and nacelle assembly will not be adversely affected by high frequency torque oscillations during unbalanced voltage supply.

Overall, the advantage in the electrical performance and structural load performance for WT-EMC has been validated during grid faults. The power electronic switches are sensitive to over voltage and over current even within short time, therefore, their overload capability is limited, which in turn limits the reactive current generated during grid faults for Type 3 and Type 4 wind turbines. Especially in case of large disturbances for Type 3 wind turbines, a protection method is necessary to protect the converter against over current, the generator rotor against over voltage and the dc-link against over voltage. The crowbar protection is commonly used, but once it is triggered, the rotor side converter is disabled and bypassed. DFIG behaves as a conventional squirrel induction generator and the independent controllability of active power and reactive power is lost. The reactive power can not only be generated but also be absorbed for the DFIG magnetization needs. In the case of WT-EMC, the synchronous generator is directly coupled with the grid and with its excellent transient overload capability is able to generate reactive current up to three times the rated current—thus offering improved voltage support and enhancing the power system stability. Furthermore, the electromagnetic coupler decouples the synchronous generator and gearbox, therefore, the synchronous generator torque oscillations cannot be transmitted to the gearbox side drive train. This can protect the wind turbine from the adverse impact of the oscillation torque and the wind turbine lifetime can be extended.

5. Conclusions

In this paper a novel variable speed wind turbine based on an electromagnetic coupler with a synchronous generator directly coupled to the grid has been proposed. The topology of this wind turbine is presented and a control strategy is proposed. In order to investigate the wind turbine voltage support capability during grid faults, a model of the wind turbine is built in Matlab/Simulink to simulate the electrical performance and is coupled to an aeroelastic model in HAWC2 code to simulate structural loads. Compared with the most common variable speed wind turbines (Type 3 and Type 4 wind turbines), the variable speed wind turbine based on electromagnetic coupler gives a better transient overload and voltage support behavior. Moreover, the electromagnetic coupler decouples the synchronous generator from the gearbox and wind turbine rotor side of the drive train, the synchronous generator oscillation torque is not transmitted through the gearbox and to the rest of the drive train and wind turbine structure during grid faults. This is a benefit for the drive train components, especially the gearbox. However, the main frame length needs to be increased and the nacelle weight becomes larger. The wind turbine drive train efficiency also becomes a little lower. Though there are challenges, compared with Type 3 and Type 4 wind turbines, the advantages of this wind turbine will become more and more obvious with the stricter and stricter grid requirements on wind turbines and wind power plants. The electromagnetic coupler used now is similar to the DFIG of similar power rating in

terms of the weight and the length is shorter. Therefore, a more compact and lighter electromagnetic coupler design is the next key step in the design of this concept.

Acknowledgments

This paper is supported by the National Basic Research Program of China (973 Program, 2013CB02708201). And the financial support provided by China Scholarship Council (CSC) during a visit of Rui You to DTU Wind Energy is acknowledged.

Conflicts of Interest

The authors declare no conflict of interest.

Appendix

The main parameters of components in the drive train of 2 MW WT-EMC and controllers are the following:

Turbine:

- rotor diameter $d = 80$ m;
- tower height $h = 80$ m.

Gearbox:

- ratio $n = 71.76$.

Electromagnetic coupler:

- nominal power $P_n = 350$ kVA;
- line-to-line voltage $V_n = 690$ V;
- frequency $f_n = 18$ Hz;
- pole pairs $p = 6$.

Synchronous generator:

- nominal power $P_n = 2.5$ MVA;
- line-to-line voltage $V_n = 690$ V;
- frequency $f_n = 50$ Hz;
- pole pairs $p = 2$.

Controllers:

- pitch angle limit: $0\text{--}90^\circ$;
- pitch rate limit: $10^\circ/\text{s}$;
- converter torque command rate limit: 0.3 pu/s.

References

1. Yamamoto, M.; Motoyoshi, O. Active and reactive power control for doubly-fed wound rotor induction generator. *IEEE Trans. Power Electron.* **1991**, *6*, 624–629.
2. Li, H.; Chen, Z. Overview of different wind generator systems and their comparisons. *IET Renew. Power Gener.* **2008**, *2*, 123–138.
3. *Electrical Simulation Models—Wind Turbines*; International Electrotechnical Commission: Geneva, Switzerland, 2013.
4. Hansen, A.D.; Sørensen, P.; Iov, F.; Blaabjerg, F. Centralised power control of wind farm with doubly fed induction generators. *Renew. Energy* **2006**, *31*, 935–951.
5. Polinder, H.; van der Pijl, F.F.A.; de Vilder, G.J.; Tavner, P.J. Comparison of direct-drive and geared generator concepts for wind turbines. *IEEE Trans. Energy Convers.* **2006**, *21*, 725–733.
6. Haque, M.E.; Negnevitsky, M.; Muttaqi, K.M. A novel control strategy for a variable-speed wind turbine with a permanent-magnet synchronous generator. *IEEE Trans. Ind. Appl.* **2010**, *46*, 331–339.
7. Tan, K.; Islam, S. Optimum control strategies in energy conversion of PMSG wind turbine system without mechanical sensors. *IEEE Trans. Energy Convers.* **2004**, *19*, 392–399.
8. Iov, F.; Hansen, A.D.; Sørensen, P.; Cutululis, N.A. *Mapping of Grid Faults and Grid Codes*; Technical University of Denmark: Roskilde, Denmark, 2007.
9. Zhou, Y.; Bauer, P.; Ferreira, J.A.; Pierik, J. Operation of grid-connected DFIG under unbalanced grid voltage condition. *IEEE Trans. Energy Convers.* **2009**, *24*, 240–246.
10. Morren, J.; de Haan, S. Ridethrough of wind turbines with doubly-fed induction generator during a voltage dip. *IEEE Trans. Energy Convers.* **2005**, *20*, 435–441.
11. Brekken, T.A.; Mohan, N. Control of a doubly fed induction wind generator under unbalanced grid voltage conditions. *IEEE Trans. Energy Convers.* **2007**, *22*, 129–135.
12. Muyeen, S.M.; Takahashi, R.; Murata, T.; Tamura, J. A variable speed wind turbine control strategy to meet wind farm grid code requirements. *IEEE Trans. Power Syst.* **2010**, *25*, 331–340.
13. Müller, H.; Pöller, M.; Basteck, A.; Tilscher, M.; Pfister, J. Grid Compatibility of Variable Speed Wind Turbines with Directly Coupled Synchronous Generator and Hydro-Dynamically Controlled Gearbox. In Proceedings of the Sixth International Workshop on Large-Scale Integration of Wind Power and Transmission Networks for Offshore Wind Farms, Delft, The Netherlands, 26–28 October 2006.
14. Chen, J.; Zhou, Q.; Chai, J.; Bi, D.; Sun, X.; Liu, W. VSCF wind turbine generator based on an electromagnetic coupler. *J. Tsinghua Univ. Sci. Tech.* **2011**, *51*, 361–366 (in Chinese).
15. You, R.; Chai, J.; Sun, X.; Li, J.; Liu, W. Experimental study of variable speed wind turbine based on electromagnetic couplers. *Proc. Chin. Soc. Electr. Eng.* **2013**, *33*, 92–98 (in Chinese).
16. Hansen, M.H.; Hansen, A.D.; Larsen, T.J.; Øye, S.; Sørensen, P.; Fuglsang, P. *Control Design for a Pitch-Regulated, Variable Speed Wind Turbine*; Technical University of Denmark: Roskilde, Denmark, 2005.
17. Chen, B. *Automatic Control System for Electric Drive*, 3rd ed.; China Machine Press: Beijing, China, 2003; pp. 190–214 (in Chinese).

18. Krause, P.C. *Analysis of Electric Machinery*; McGraw-Hill: New York, NY, USA, 1986; pp. 133–160.
19. 421.5-1992—IEEE Recommended Practice for Excitation System Models for Power System Stability Studies; IEEE Power & Energy Society: Piscataway, NJ, USA, 1992.
20. Larsen, T.J.; Hansen, A.M. *How 2 HAWC2, the User's Manual*; Technical University of Denmark: Roskilde, Denmark, 2012.
21. Larsen, T.J.; Madsen, H.A.; Larsen, G.C.; Hansen, K.S. Validation of the dynamic wake meander model for loads and power production in the Egmond aan Zee Wind Farm. *Wind Energy* **2013**, *16*, 605–624.
22. *Grid Code High and Extra High Voltage*; E.ON Netz GmbH: Bayreuth, Germany, 2006.
23. Barahona, B.; Cutululis, N.A.; Hansen, A.D.; Sørensen, P. Unbalanced voltage faults: The impact on structural loads of doubly fed asynchronous generator wind turbines. *Wind Energy* **2013**, doi:10.1002/we.1621.

© 2013 by the authors; licensee MDPI, Basel, Switzerland. This article is an open access article distributed under the terms and conditions of the Creative Commons Attribution license (<http://creativecommons.org/licenses/by/3.0/>).